Imaging nuclei by smashing them

Jiangyong Jia

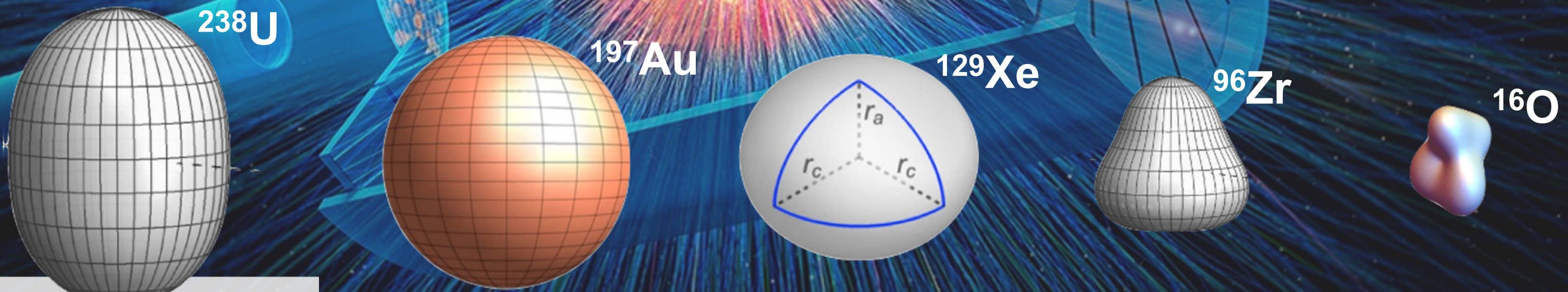

Stony Brook University

Jan 16, 2025 ATHIC Berhampur, Odisha, India

Traditional imaging method

Coherent diffraction

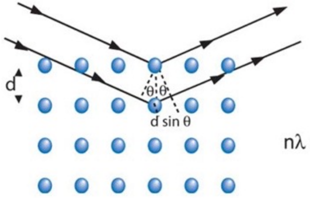

$n\lambda = 2\,d\sin\theta$

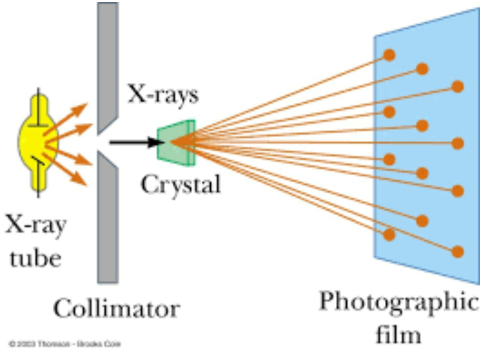

Inverse Fourier transform

$$\rho(xyz) = \frac{1}{V}\sum_{hkl\,-\infty}^{+\infty} \underbrace{|F(hkl)|}_{\text{Amplitudes}} \cdot e^{-2\pi i[hx+ky+lz-\overbrace{\phi(hkl)}^{\text{Phases}}]}$$

Traditional imaging method

Coherent diffraction

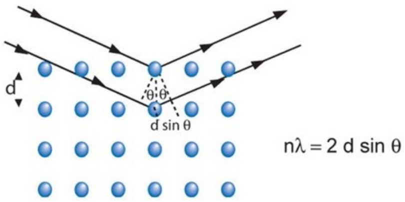

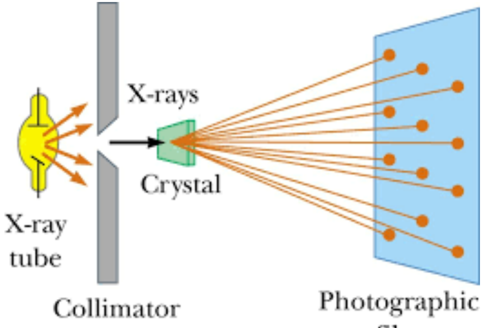

Inverse Fourier transform

$$\rho(xyz) = \frac{1}{V}\sum_{hkl\,-\infty}^{+\infty} |F(hkl)| \cdot e^{-2\pi i[hx+ky+lz-\phi(hkl)]}$$

Amplitudes Phases

$$\gamma + \underset{\mathrm{Au}}{\mathrm{p}} \rightarrow J/\psi + \underset{\mathrm{Au}}{\mathrm{p}}$$

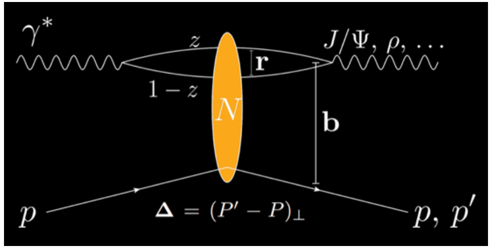

Sensitive to the averaged structure of the p/Au

$$\frac{d\sigma^{\gamma^* p \to Vp}}{dt} = \frac{1}{16\pi}\left|\left\langle A^{\gamma^* p\to Vp}\left(x_P, Q^2, \vec{\Delta}\right)\right\rangle\right|^2$$

$$A \sim \int d^2b\, dz\, d^2r\, \psi^*\psi^V(\vec{r}, z, Q^2) e^{-i(\vec{b}-(\frac{1}{2}-z)\vec{r})\cdot\vec{\Delta}} N(\vec{r}, x, \vec{b})$$

Image taken before destruction

Imaging by smashing: some examples

Smashing a deformed droplet on surface

$$F = \nabla P$$

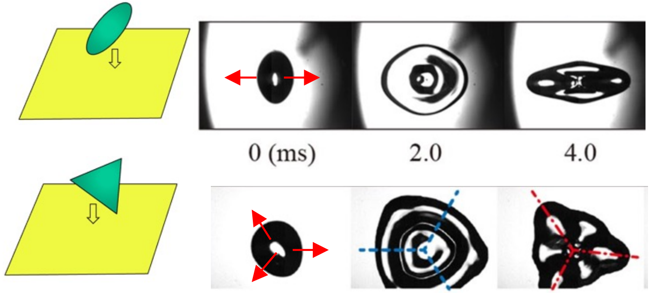

strongly-coupled cold atomic gas

$$L_{mfp} = 1/\rho\sigma$$

Science 298, 2179 (2002)

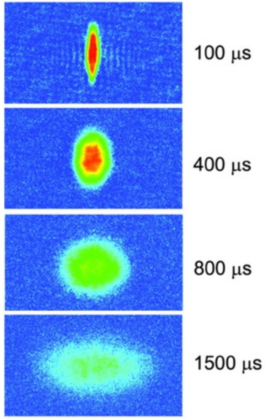

Coulomb Explosion Imaging in Chemistry

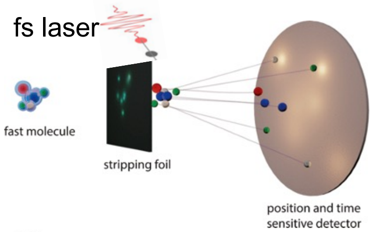

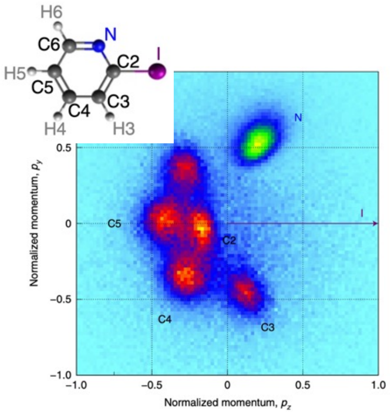

Instantaneous stripping of electrons and let atoms explode under mutual coulomb repulsion

Imaging by smashing: some examples

Smashing a deformed droplet on surface

$$F = \nabla P$$

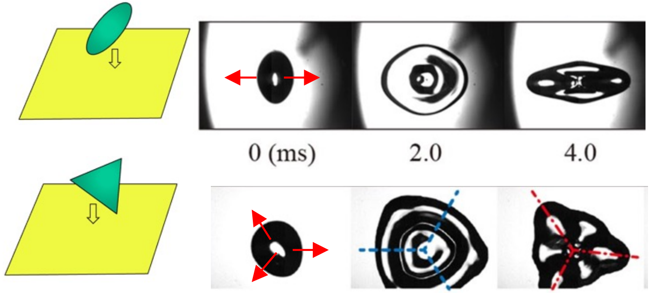

strongly-coupled cold atomic gas

$$L_{mfp} = 1/\rho\sigma$$

Science 298, 2179 (2002)

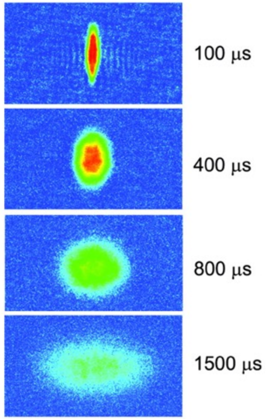

Coulomb Explosion Imaging in Chemistry

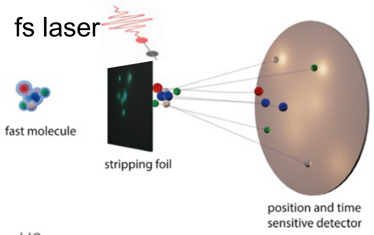

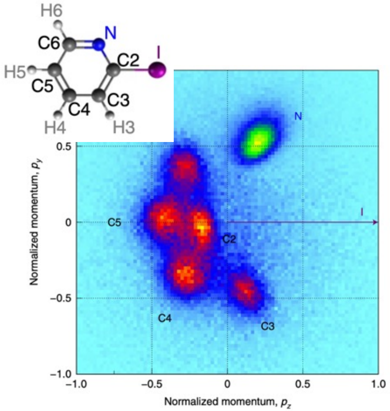

EOS, viscosity…

$$T_{\mu\nu}(\tau = 0) \qquad \partial_\mu T^{\mu\nu} = 0 \qquad T_{\mu\nu}(\tau = \infty)$$

snapshot → evolution → measurement

Image inferred after destruction

Instantaneous stripping of electrons and let atoms explode under mutual coulomb repulsion

Imaging by smashing: high-energy collisions

Take a snapshot — **Evolution** — **Measurement**

nuclei

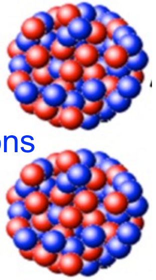

400 nucleons

$T_{\mu\nu}(\tau=0)$

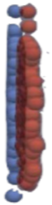

$\tau \sim 2R_0/\Gamma \sim 0.1\mathrm{fm}/c$

exposure

Pressure-driven expansion of quark-gluon plasma (QGP) →

$\partial_\mu T^{\mu\nu}=0$, EOS, viscosity…

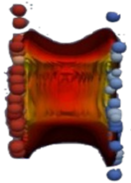

$\tau \sim 10\mathrm{fm}/c$

expansion

free-streaming →

$T_{\mu\nu}(\tau=\infty)$

30,000 particles

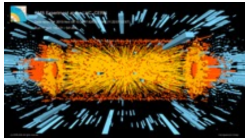

$\tau \sim 10^{15}\ \mathrm{fm}/c$

detection

Large entropy production enable a semi-classical description

- Initial condition is a fast snapshot of nuclear structure (<0.1fm/c)
- Transformed to the final state via hydrodynamic expansion (EFT)
- Reverse-engineer to infer the snapshot, aided by large information output

Ability to image ←→ Understanding of the QGP

Imaging by smashing: high-energy collisions

Take a snapshot

nuclei

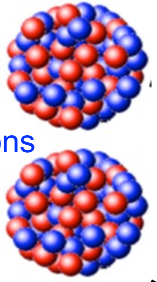

400 nucleons

$T_{\mu\nu}(\tau=0)$

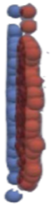

$\tau \sim 2R_0/\Gamma \sim 0.1 \mathrm{fm}/c$

exposure

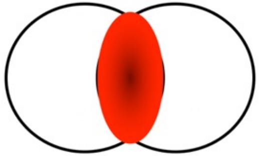

$R_\perp^2 \propto \langle r_\perp^2 \rangle$, $\mathcal{E}_n \propto \langle r_\perp^n e^{in\phi} \rangle$

size & shape

Evolution

$\partial_\mu T^{\mu\nu}=0$, EOS, viscosity…

Pressure-driven expansion of quark-gluon plasma (QGP)

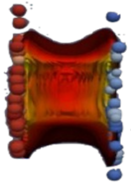

$\tau \sim 10 \mathrm{fm}/c$

expansion

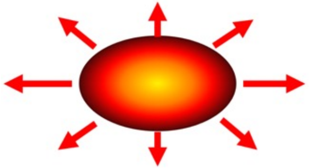

$$\frac{d^2N}{d\phi dp_T} = N(p_T)\left(\sum_n V_n\, e^{-in\phi}\right)$$

observables

Measurement

free-streaming

$T_{\mu\nu}(\tau=\infty)$

30,000 particles

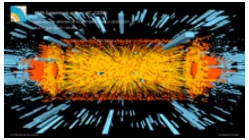

$\tau \sim 10^{15}\ \mathrm{fm}/c$

detection

Event-by-event linear responses:

$$V_n \propto \mathcal{E}_n$$

$$\frac{\delta[p_T]}{[p_T]} \propto -\frac{\delta R_\perp}{R_\perp}$$

Preserving the snapshot to the final state

Several real event display at LHC $T_{\mu\nu}(\tau = \infty)$

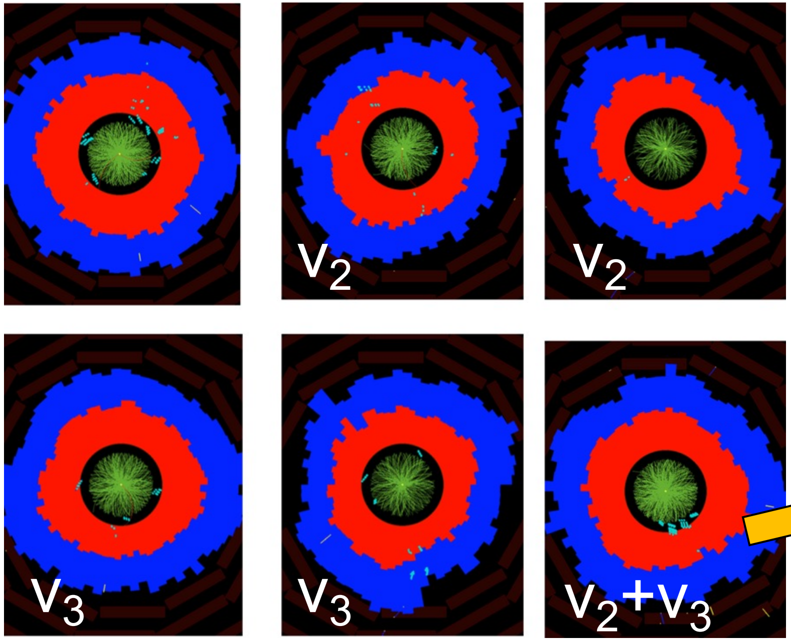

One event

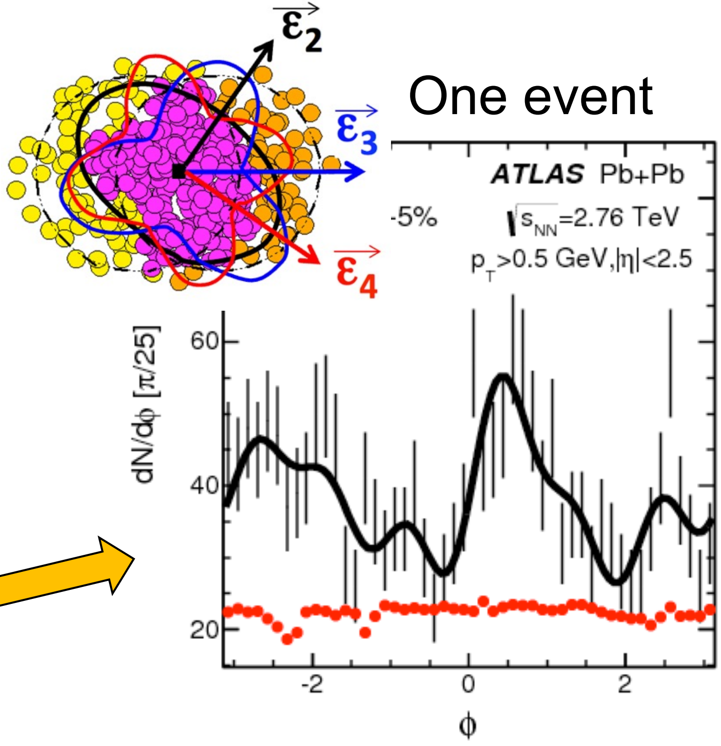

higher-order harmonics seen at single event level

Seems we can infer the initial condition of QGP, which carries imprints of the colliding nuclei.

But what kinds of images do we expect to get?

Atomic nuclei at low energy

Many-body quantum systems, govern by short-range strong nuclear force
Emergent properties in between discrete nucleon and bulk nuclear matter, like quantum dot.
Configuration is one that minimizes E, which is often deformed away from magic numbers

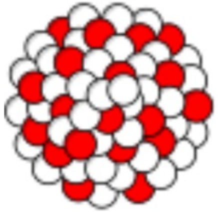

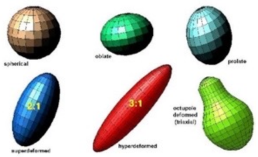

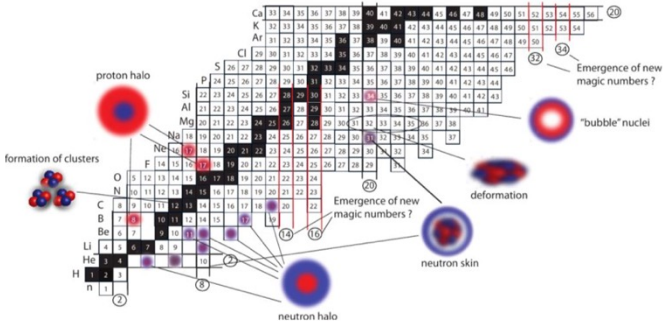

β2-landscape

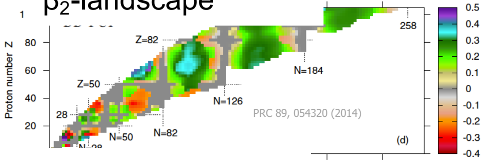

β3-landscape

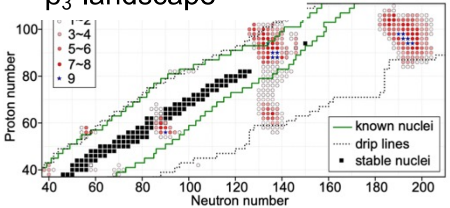

$$\rho(r,\theta,\phi) = \frac{\rho_0}{1+e^{(r-R(\theta,\phi))/a_0}}$$

$$R(\theta,\phi) = R_0(1+\beta_2[\cos\gamma Y_{2,0}(\theta,\phi)+\sin\gamma Y_{2,2}(\theta,\phi)]+\beta_3 Y_{3,0}(\theta,\phi)+\beta_4 Y_{4,0}(\theta,\phi))$$

$0 \le \gamma \le \pi/3$

Very rich landscape of shapes and other structures

Nuclear shapes at low energy: long exposure

Each DOF has zero-point fluctuations within certain timescale.

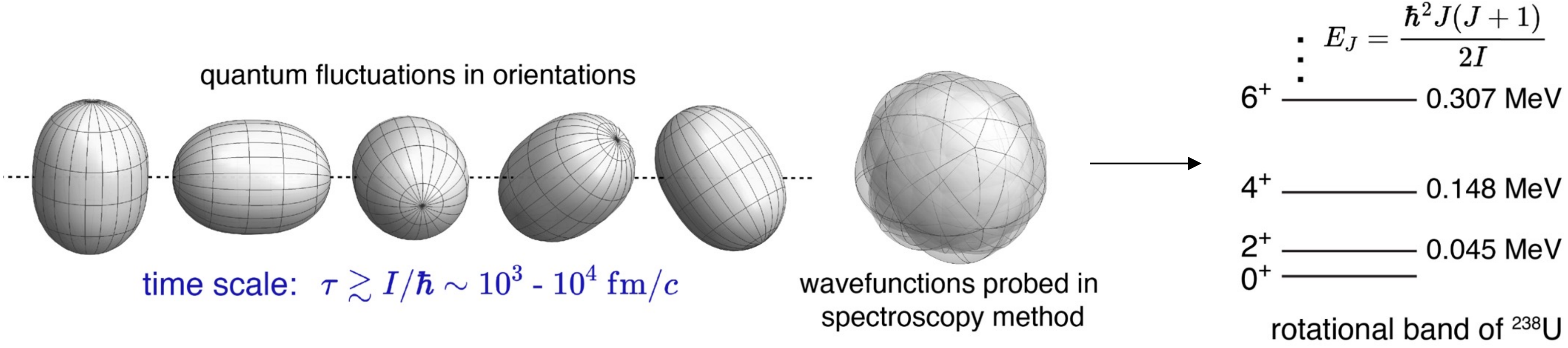

Spectroscopic methods probe a superposition of these fluctuations

Instantaneous shapes not directly seen→ intrinsic shape not observable at low E

Infer shape from model comparison to energy-transition-lifetime measurements.

Nuclear shape at high-energy: smashing experiment

To see event-by-event shape directly, one must have access to instantaneous many-body correlations $\Psi\left(\mathbf{r}_1, \mathbf{r}_2 \ldots\right)$

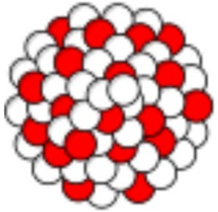

τ_{expo}

We will see all DOFs longer than this timescale: $\tau > \tau_{\text{expo}}$

Nucleons, hadrons, quark, gluons, gluon saturations

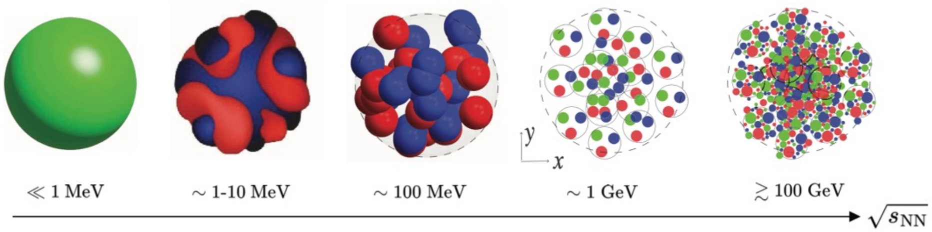

Concept of shape is collision energy dependent

$\epsilon_2 = 0$ $\qquad$ $\epsilon_2 \sim \frac{1}{\sqrt{A}}$

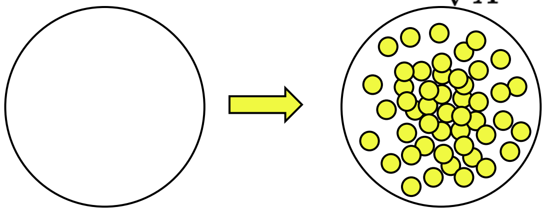

Spherical Woods-saxon $\qquad$ Sampled with A nucleons

$$\epsilon_2 = \underbrace{\epsilon_0}_{} + \underbrace{p(\Omega)\beta_2}_{} + \mathcal{O}\left(\beta_2^2\right)$$

$\sqrt{s}$-dependent quantum fluctuation induced shape

Global shape rotational vibrational

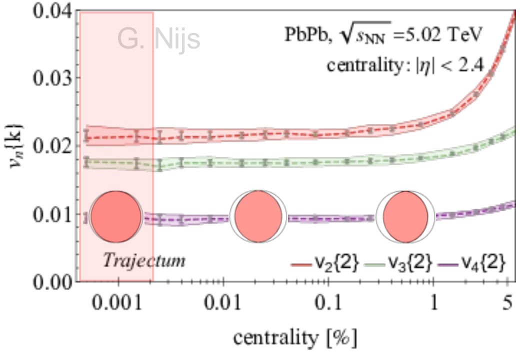

Smashing experiment and nuclear structure

Nuclear Structure

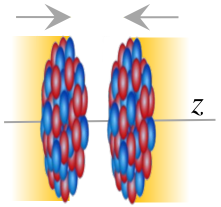

$$T_A(x,y) = \int \rho(x,y,z)dz$$

Shape and radial dis.

- $\beta_2 \rightarrow$ Quadrupole deformation
- $\beta_3 \rightarrow$ Octupole deformation
- $a_0 \rightarrow$ Surface diffuseness
- $R_0 \rightarrow$ Nuclear size

….
Nucleon width
Nucleon distance
substructure

Energy deposition

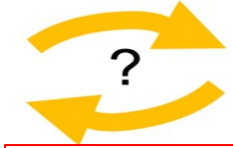

$$T \propto \left(\frac{T_A^p + T_B^p}{2}\right)^{q/p}$$

Initial condition

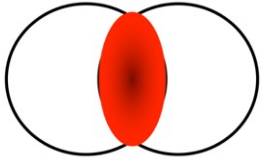

Size & shape

$$R_\perp^2 \propto \langle r_\perp^2 \rangle,\ \mathcal{E}_n \propto \langle r_\perp^n e^{in\phi} \rangle$$

hydrodynamics

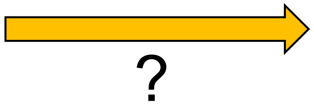

Final state

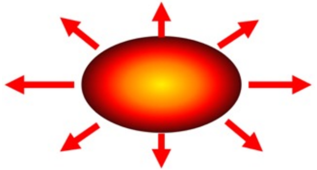

Observables

$$\frac{d^2N}{d\phi dp_T} = N(p_T)\left(\sum_n V_n\, e^{-in\phi}\right)$$

Precision of imaging method {
- space-time dynamics of QGP
- energy deposition mechanism

How to apply the method in practice?

Impact of deformation: head-on collisions

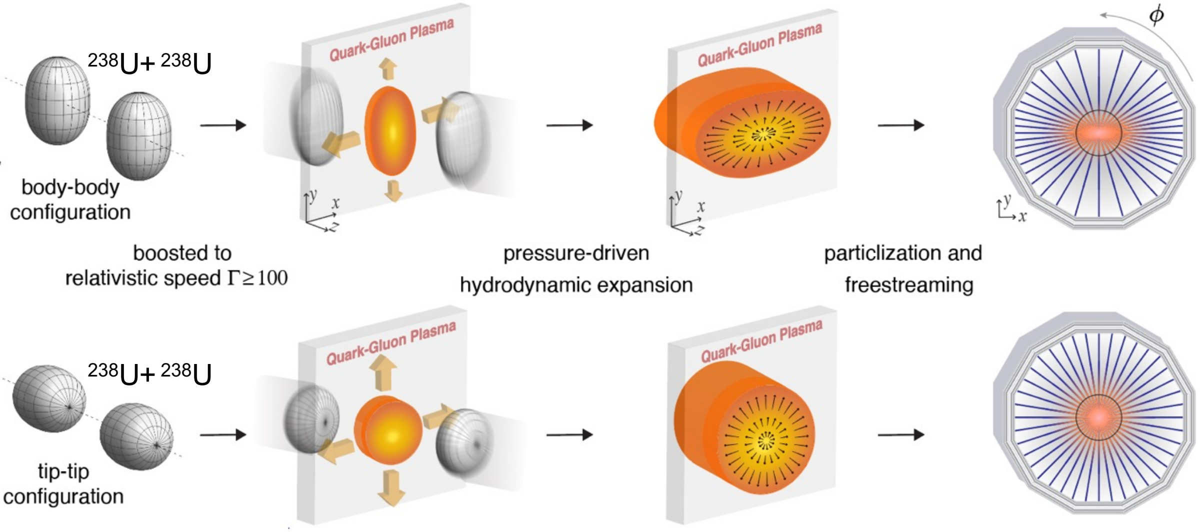

Collision geometry depends on the orientations: head-on collisions has two extremes body-body or tip-tip collisions

Body-body: large eccentricity large size

$v_2 \nearrow \quad p_T \searrow$

Tip-tip : small eccentricity small size

$v_2 \searrow \quad p_T \nearrow$

- Deformation enhances the fluctuations of v_2 and $[p_T]$.
- and leads to anti-correlation between v_2 and $[p_T]$.

$^{238}U + ^{238}U$

$$\langle v_2^2 \rangle = a_1 + b_1 \beta_2^2 \,,$$
$$\langle (\delta p_T)^2 \rangle = a_2 + b_2 \beta_2^2 \,,$$
$$\langle v_2^2 \delta p_T \rangle = a_3 - b_3 \beta_2^3 \cos(3\gamma)$$

Impact of deformation: head-on collisions

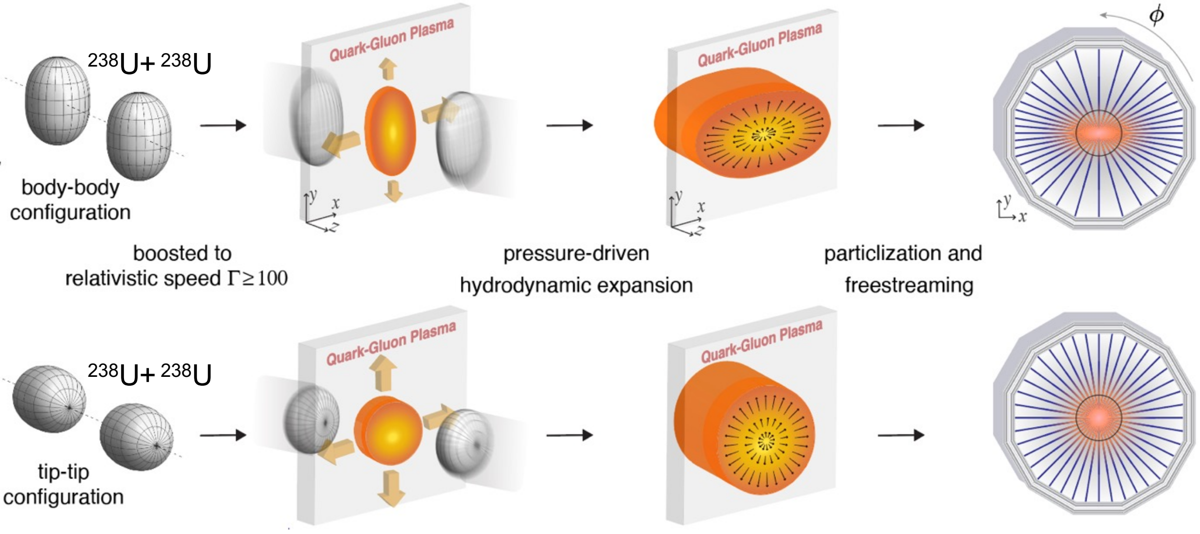

Collision geometry depends on the orientations: head-on collisions has two extremes body-body or tip-tip collisions

Body-body: large eccentricity large size

$v_2\nearrow$ $p_T\searrow$

Tip-tip : small eccentricity small size

$v_2\searrow$ $p_T\nearrow$

^{197}Au+ ^{197}Au

^{238}U+ ^{238}U

$$\langle v_2^2 \rangle = a_1 + b_1 \beta_2^2 ,$$
$$\langle (\delta p_T)^2 \rangle = a_2 + b_2 \beta_2^2 ,$$
$$\langle v_2^2 \delta p_T \rangle = a_3 - b_3 \beta_2^3 \cos(3\gamma)$$

- Deformation enhances the fluctuations of v_2 and $[p_T]$.
- and leads to anti-correlation between v_2 and $[p_T]$.
- Compare to collision of near spherical ^{197}Au

Compare two systems to disentangle global deformation and quantum fluctuation!

low E

high E

Impact of deformation: head-on collisions

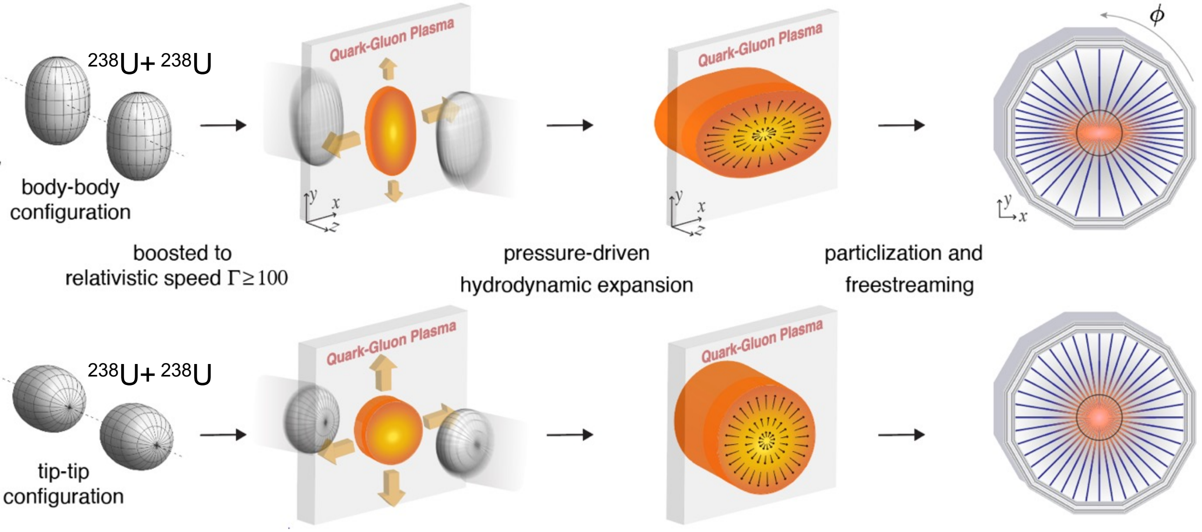

Collision geometry depends on the orientations: head-on collisions has two extremes body-body or tip-tip collisions

Body-body: large eccentricity large size

$v_2 \nearrow \quad p_T \searrow$

Tip-tip : small eccentricity small size

$v_2 \searrow \quad p_T \nearrow$

UU/AuAu ratios:

$$R_{\langle v_2^2 \rangle} \approx 1 + \frac{b_1}{a_1} \beta_2^2 \,,$$

$$R_{\langle (\delta p_{\mathrm{T}})^2 \rangle} \approx 1 + \frac{b_2}{a_2} \beta_2^2 \,,$$

$$R_{\langle v_2^2 \delta p_{\mathrm{T}} \rangle} \approx 1 - \frac{b_3}{a_3} \beta_2^3 \cos(3\gamma)$$

- Deformation enhances the fluctuations of v_2 and $[p_T]$.
- and leads to anti-correlation between v_2 and $[p_T]$.
- Compare to collision of near spherical ^{197}Au

Compare two systems to disentangle global deformation and quantum fluctuation!

low E　　　　high E

Ratio of observables $R_{\mathcal{O}} = \langle\mathcal{O}\rangle_{\mathrm{U+U}} / \langle\mathcal{O}\rangle_{\mathrm{Au+Au}}$

$$R_{\langle v_2^2\rangle} \approx 1 + \frac{b_1}{a_1}\beta_2^2\,,$$
$$R_{\langle(\delta p_{\mathrm{T}})^2\rangle} \approx 1 + \frac{b_2}{a_2}\beta_2^2\,,$$
$$R_{\langle v_2^2\delta p_{\mathrm{T}}\rangle} \approx 1 - \frac{b_3}{a_3}\beta_2^3\cos(3\gamma)$$

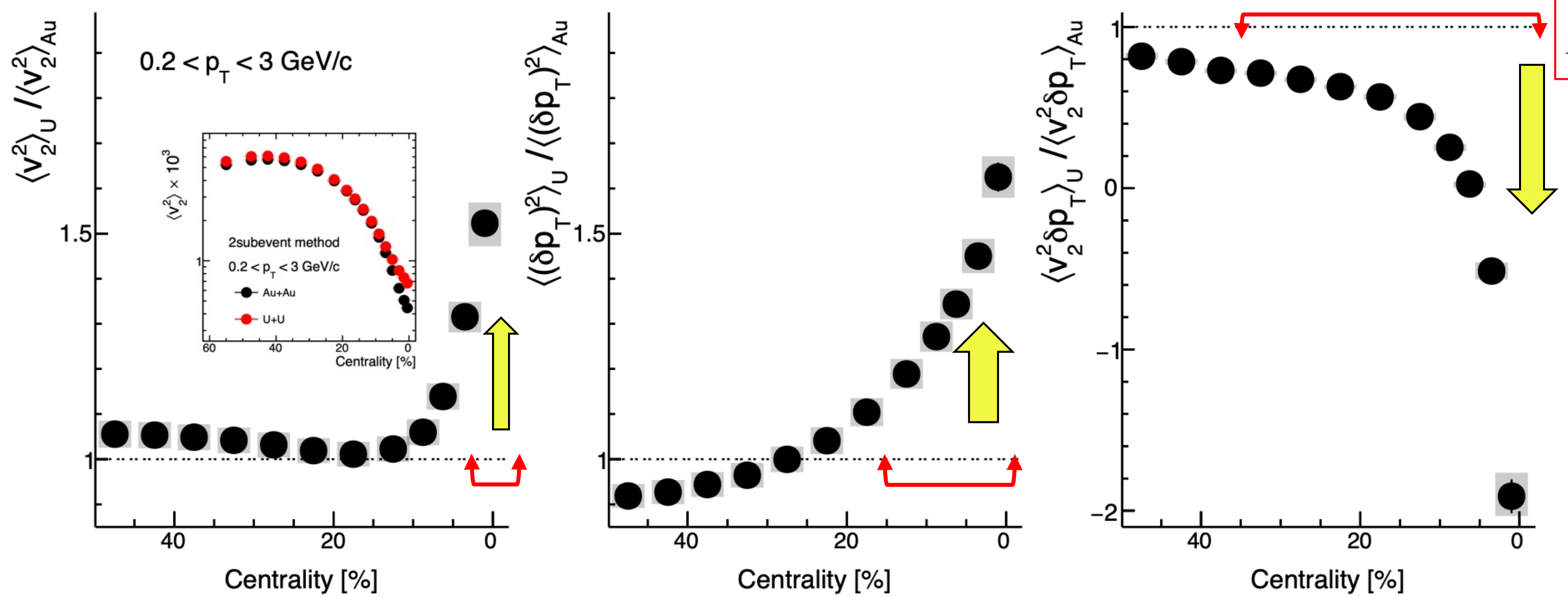

Ratios cancel final state effects and isolate the effects of initial state/nuclear structures!

U deformation dominates the ultra-central collisions (UCC)
→50%-70% impact on $<(\delta p_T)^2>$ and $<v_2^2>$, 300% for $<v_2^2\delta p_T>$

More smooth centrality dependence for $<(\delta p_T)^2>$ than $<v_2^2>$
→v_2 is dominated by v_2^{RP} (unaffected by deformation), having residual impact in UCC

Compared to hydrodynamic models

$$R_{\langle v_2^2\rangle} \approx 1 + \frac{b_1}{a_1}\beta_2^2 ,$$

$$R_{\langle(\delta p_T)^2\rangle} \approx 1 + \frac{b_2}{a_2}\beta_2^2 ,$$

$$R_{\langle v_2^2 \delta p_T\rangle} \approx 1 - \frac{b_3}{a_3}\beta_2^3 \cos(3\gamma)$$

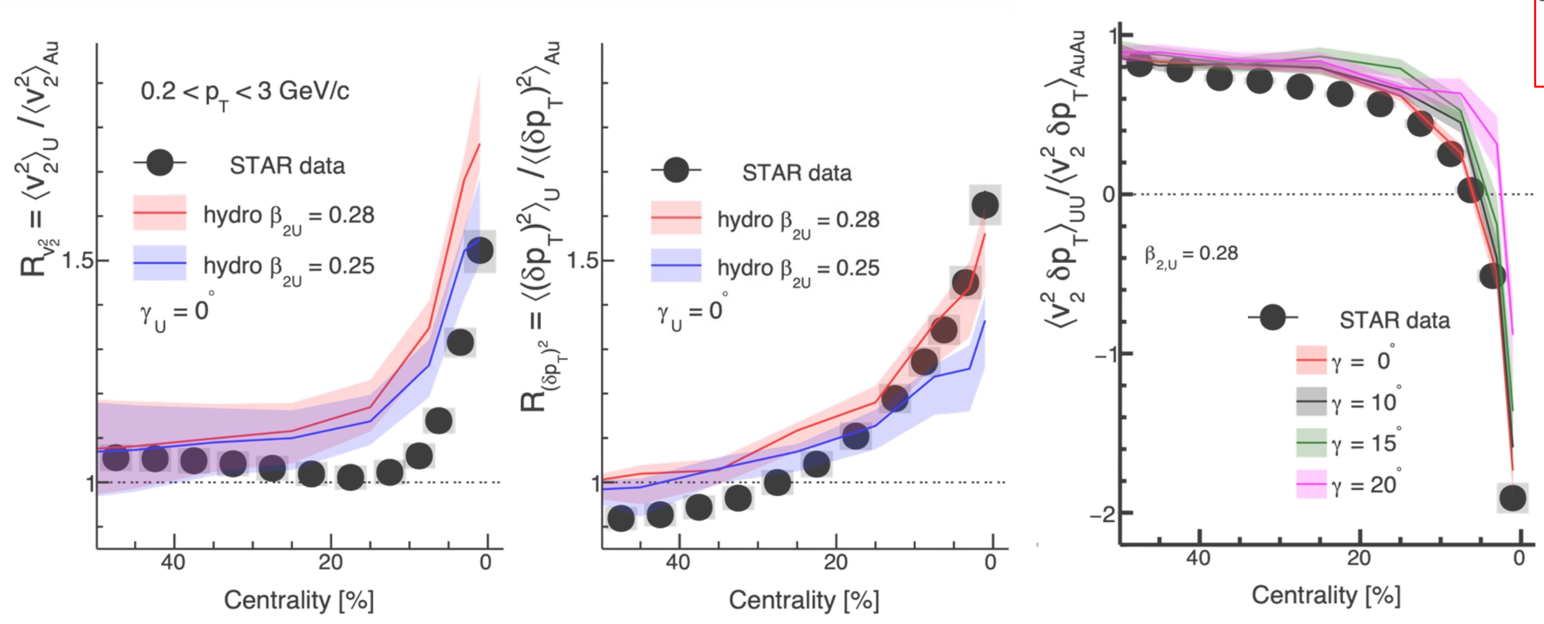

Compare with state-of-the-art ipglasma+music+UrQMD hydro model.

The $\langle(\delta p_T)^2\rangle$ and $\langle v_2^2 \delta p_T\rangle$ data seems prefers value closer to β_{2U} =0.28 and a small γ_U.

$\langle v_2^2\rangle$ prefer a smaller β_{2U} value

Constraining the U238 shape

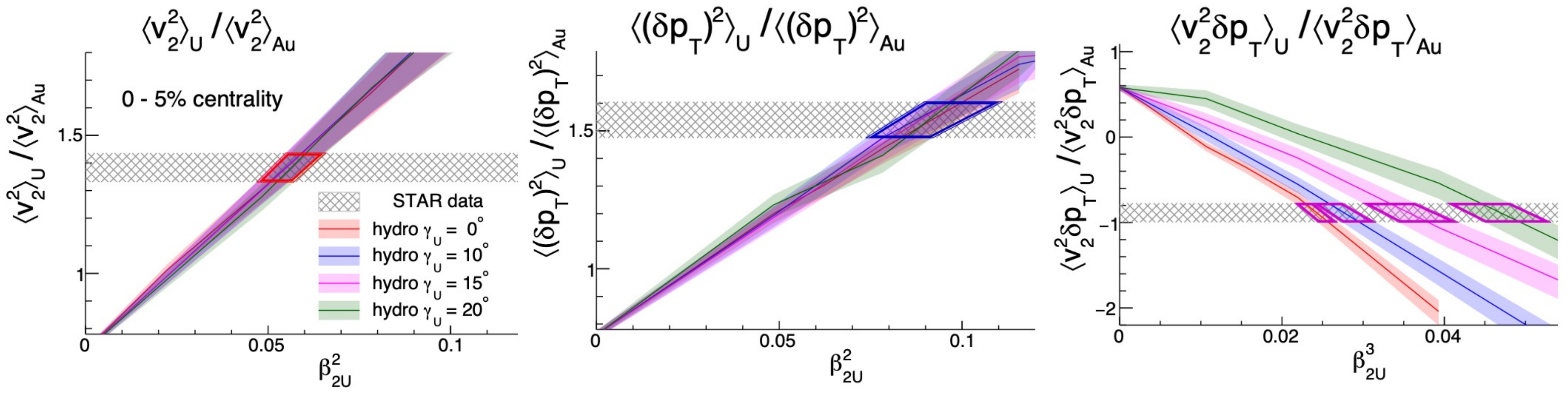

Confirming these relations, including strong sensitivity to triaxiality

focus on $\langle(\delta p_{\mathrm{T}})^2\rangle$, $\langle v_2^2 \delta p_{\mathrm{T}}\rangle$

$$R_{\langle v_2^2\rangle} \approx 1 + \frac{b_1}{a_1}\beta_2^2 \,,$$

$$R_{\langle(\delta p_{\mathrm{T}})^2\rangle} \approx 1 + \frac{b_2}{a_2}\beta_2^2 \,,$$

$$R_{\langle v_2^2 \delta p_{\mathrm{T}}\rangle} \approx 1 - \frac{b_3}{a_3}\beta_2^3 \cos(3\gamma)$$

Results

High-energy estimate

$$\beta_{2U} = 0.286 \pm 0.025$$

$$\gamma_{\mathrm{U}} = 8.7^\circ \pm 4.5^\circ$$

Hydro-model uncertainties dominate

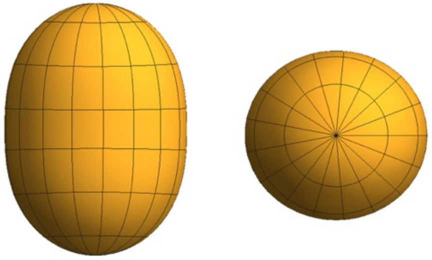

x-z x-y

Low-energy estimate

$$\beta_{2U} = 0.287 \pm 0.007$$

$$\gamma_{\mathrm{U}} \sim 6^\circ - 8^\circ$$

With liquid model assumption

$$\frac{\left\langle (\delta p_T)^2 \right\rangle_{\mathrm{U}}}{\left\langle (\delta p_T)^2 \right\rangle_{\mathrm{Au}}} \approx \frac{a_2 + b_2 \beta_{2U}^2}{a_2} = 1 + \frac{b_2}{a_2} \beta_{2U}^2$$

Global nuclear shape (b_2)

Spherical baseline, mainly from nucleon fluctuations. Described well by hydro model (a_2)

Deposition mechanism has weak energy dependence

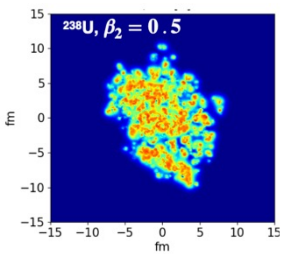

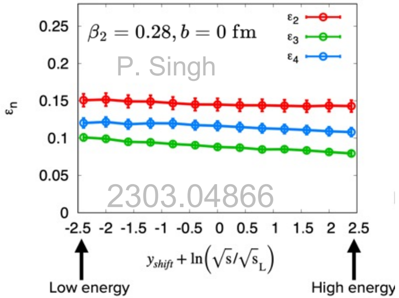

nature > article > arti

Published on Nov 6 2024

Article metrics | Last updated: Wed, 15 Jan 2025 12:52:29 Z

Imaging shapes of atomic nuclei in high-energy nuclear collisions

Access & Citations

https://doi.org/10.1038/s41586-024-08097-2

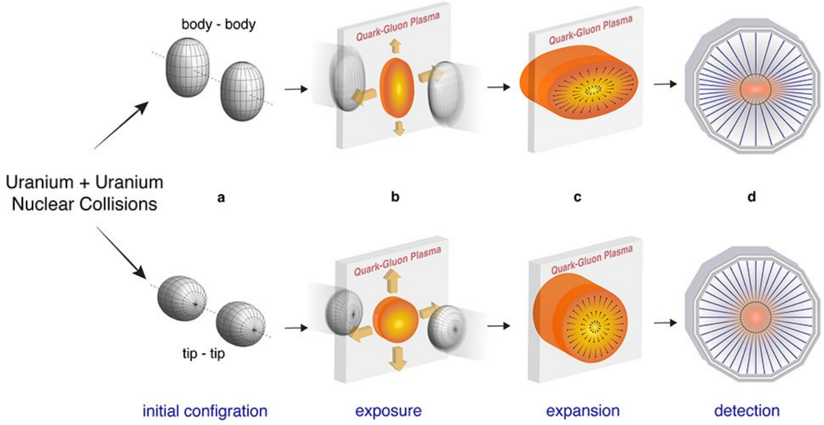

https://www.bnl.gov/newsroom/news.php?a=122119

nature

Explore content | About the journal | Publish with us | Subscribe

nature > news & views > article

https://doi.org/10.1038/d41586-024-03466-3

NEWS AND VIEWS | 06 November 2024

Rare snapshots of a kiwi-shaped atomic nucleus

Smashing uranium-238 ions together proves to be a reliable way of imaging their nuclei. High-energy collision experiments reveal nuclear shapes that are strongly elongated and have no symmetry around their longest axis.

By Magda Zielińska & Paul E. Garrett

NEWS | 06 November 2024

Smashing atomic nuclei together reveals their elusive shapes

A method to take snapshots of exploding nuclei could hold clues about the fundamental properties of gold, uranium and other elements.

By Elizabeth Gibney

https://www.nature.com/articles/d41586-024-03633-6

A general strategy for nuclear shape imaging

Flow observable = k ⊗ initial condition (structure)

QGP response,
a smooth function of N+Z

Structure of colliding nuclei,
non-monotonic function of N and Z

Compare two systems X and Y of same mass but different structure

$$\rho(r,\theta,\phi) \propto \frac{1}{1+e^{(r-R(\theta,\phi))/a}}$$

$$R_{\mathcal{O}} \equiv \frac{\mathcal{O}_{\mathrm{X+X}}}{\mathcal{O}_{\mathrm{Y+Y}}} \approx 1 + c_1\Delta\beta_2^2 + c_2\Delta\beta_3^2 + c_3\Delta R_0 + c_4\Delta a$$

arXiv: 2111.15559

Deviation from unity due to their structural differences

c_1 - c_4 directly probes energy deposition mechanism in the initial condition!

Isobar ^{96}Ru+^{96}Ru and ^{96}Zr+^{96}Zr collisions at RHIC 200 GeV

QM2022 poster, Chunjian Zhang

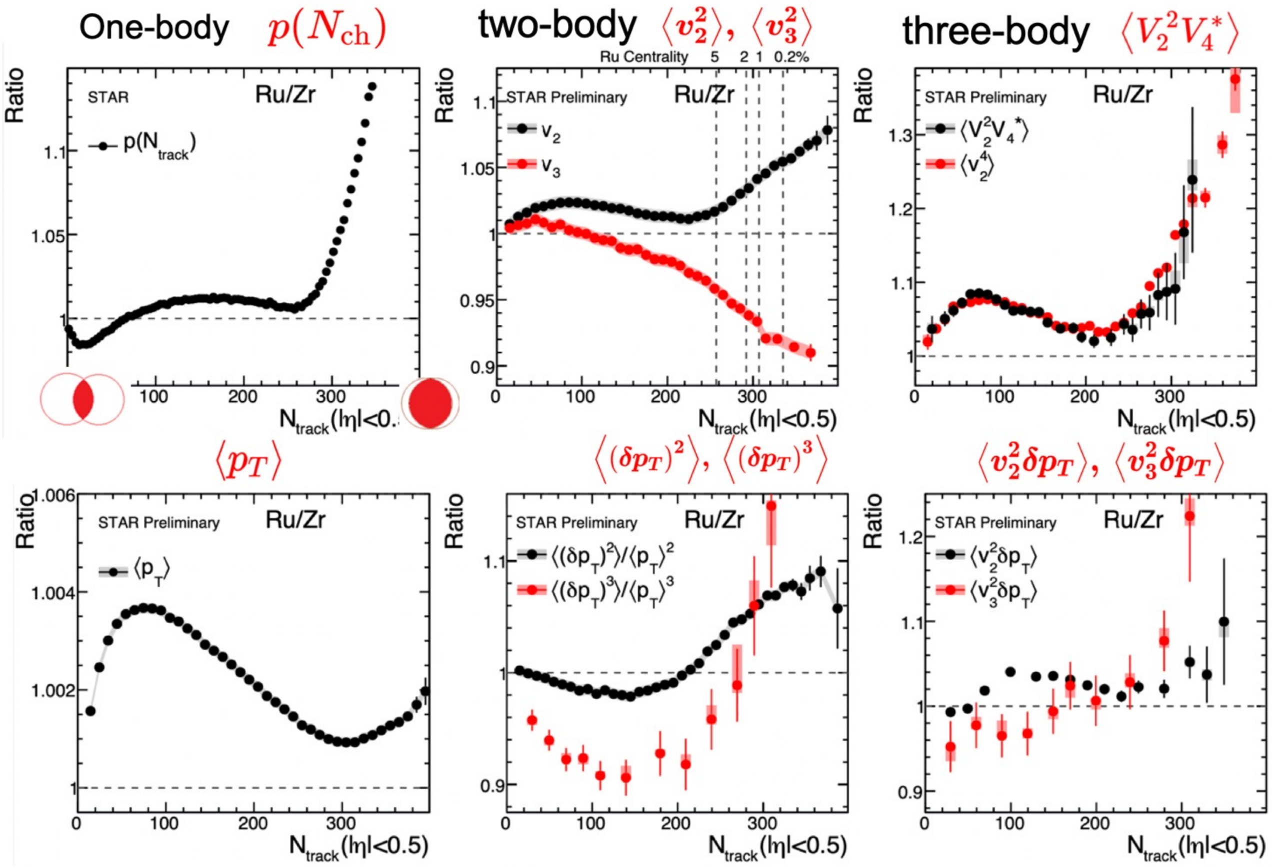

$$R_{\mathcal{O}} \equiv \frac{\mathcal{O}_{\mathrm{Ru}}}{\mathcal{O}_{\mathrm{Zr}}}$$

Structure influences everywhere

Opportunity for precision structure study

Nuclear structure via v_2-ratio and v_3-ratio

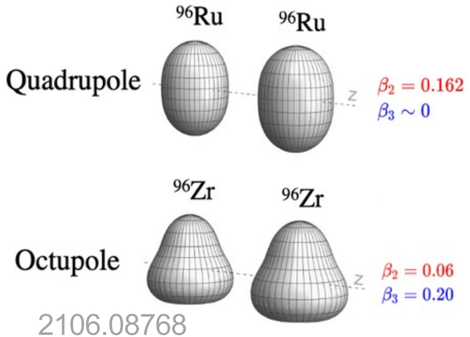

2106.08768

Species	β_2	β_3	a_0	R_0
Ru	0.162	0	0.46 fm	5.09 fm
Zr	0.06	0.20	0.52 fm	5.02 fm
difference	$\Delta\beta_2^2$	$\Delta\beta_3^2$	Δa_0	ΔR_0
	0.0226	-0.04	-0.06 fm	0.07 fm

- β_{2Ru} ~ 0.16 increase v_2, no influence on v_3 ratio
- β_{3Zr} ~ 0.2 decrease v_2 and v_3 ratio
- Δa_0 = -0.06 fm increase v_2 mid-central,
- Radius ΔR_0 = 0.07 fm slightly affects v_2 and v_3 ratio.

Is ^{96}Zr octupole deformed?

$$R_{\mathcal{O}} \equiv \frac{\mathcal{O}_{\mathrm{Ru}}}{\mathcal{O}_{\mathrm{Zr}}} \approx 1 + c_1\Delta\beta_2^2 + c_2\Delta\beta_3^2 + c_3\Delta R_0 + c_4\Delta a$$

2109.00131

Simultaneously constrain four structure parameters

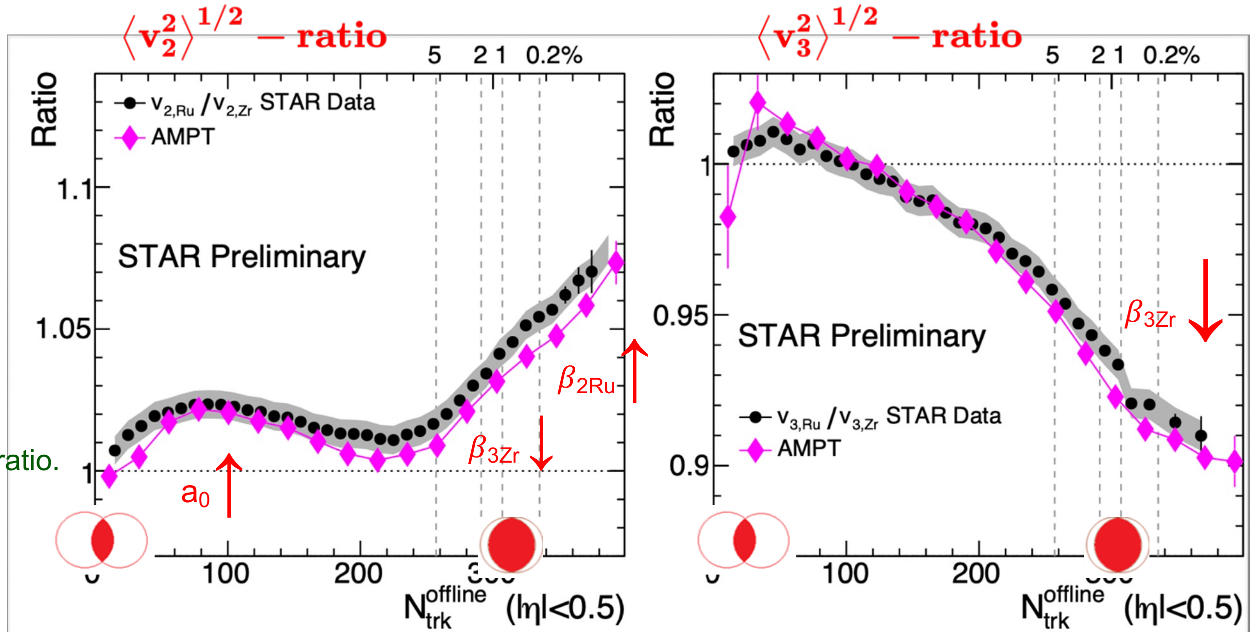

Currently available collision systems

RHIC $\sqrt{s}$=200GeV		LHC $\sqrt{s}$=5000 GeV
^{197}Au+^{197}Au vs ^{238}U+^{238}U β_{2U} γ_U β_{3U} β_{4U}	**Establish methodology** • Large sensitivity	^{129}Xe+^{129}Xe vs ^{208}Pb+^{208}Pb β_{2Xe} γ_{Xe} Neutron skin
^{96}Ru+^{96}Ru vs ^{96}Zr+^{96}Zr β_{2Ru} β_{3Zr} large skin	**Establish precision** • 0.2% measurement error vs 5-15% signal • High-order observables	
d+^{197}Au vs ^{16}O+^{16}O	**Structure of light nuclei** • Cluster, subnucleon structure. • Benchmark ab-initio models	^{16}O+^{16}O vs ^{20}Ne+^{20}Ne?
p+p, p+^{27}Al, p+^{197}Au,^{3}He+^{197}Au, ^{63}Cu+^{63}Cu, ^{63}Cu+^{197}Au	What can we learn from these?	p+p, p+^{16}O, p+^{208}Pb

What other species to consider & what questions do they answer?

Future opportunities

High-energy: fast snapshot of nucleon distribution for any collision species.

Low-energy: complexity & interpretation depends on location in nuclide chart

constrain initial condition via
nuclei with known structure

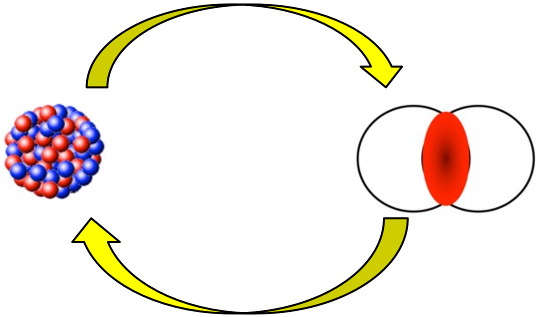

Constrain the structure for nuclei of interest
once initial condition is calibrated

Better constrains on properties of QGP

Current extraction of QGP properties
are limited by the initial condition

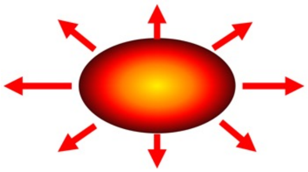

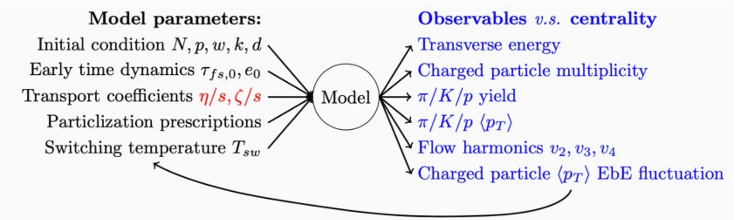

effective for discerning shape differences between isobar-like species

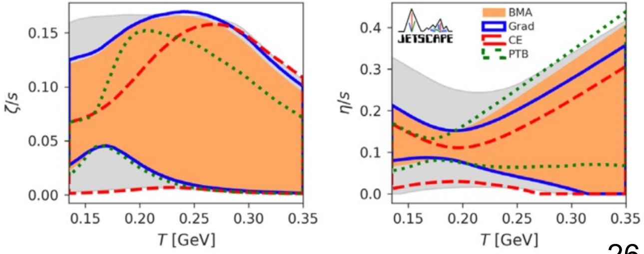

With the polished imaging-by-smashing tool,
many exciting applications lie ahead

Summary

- Imaging-by-smashing is a discovery tool for low- and high-energy nuclear physics.
- Low- and high-energy techniques together enable study of evolution of nuclear structure across energy and time scales.
- Future research should conduct collider experiments with selected isobaric pairs

2102.08158

A	isobars	A	isobars	A	isobars	A	isobars	A	isobars	A	isobars
36	Ar, S	80	Se, Kr	106	Pd, Cd	124	Sn, Te, Xe	148	Nd, Sm	174	Yb, Hf
40	Ca, Ar	84	Kr, Sr, Mo	108	Pd, Cd	126	Te, Xe	150	Nd, Sm	176	Yb, Lu, Hf
46	Ca, Ti	86	Kr, Sr	110	Pd, Cd	128	Te, Xe	152	Sm, Gd	180	Hf, W
48	Ca, Ti	87	Rb, Sr	112	Cd, Sn	130	Te, Xe, Ba	154	Sm, Gd	184	W, Os
50	Ti, V, Cr	92	Zr, Nb, Mo	113	Cd, In	132	Xe, Ba	156	Gd,Dy	186	W, Os
54	Cr, Fe	94	Zr, Mo	114	Cd, Sn	134	Xe, Ba	158	Gd,Dy	187	Re, Os
64	Ni, Zn	96	Zr, Mo, Ru	115	In, Sn	136	Xe, Ba, Ce	160	Gd,Dy	190	Os, Pt
70	Zn, Ge	98	Mo, Ru	116	Cd, Sn	138	Ba, La, Ce	162	Dy,Er	192	Os, Pt
74	Ge, Se	100	Mo, Ru	120	Sn, Te	142	Ce, Nd	164	Dy,Er	196	Pt, Hg
76	Ge, Se	102	Ru, Pd	122	Sn, Te	144	Nd, Sm	168	Er,Yb	198	Pt, Hg
78	Se, Kr	104	Ru, Pd	123	Sb, Te	146	Nd, Sm	170	Er,Yb	204	Hg, Pb

Shape Coexistence Workshop - 2023